MODELLING OF INFLUENCE OF TURBULENT TRANSITION ON HEAT TRANSFER CONDITIONS

KRZYSZTOF BOCHON, WŁODZIMIERZ WRÓBLEWSKI AND SŁAWOMIR DYKAS

Institute of Power Engineering and Turbomachinery,
Silesian University of Technology,
Konarskiego 18, 44-100 Gliwice, Poland
krzysztof.bochon@polsl.pl

(Received 30 June 2008)

Abstract: This article deals with the turbulent transition phenomenon modelling and its influence on heat transfer. The purpose of the analyses was to verify the transition modelling implemented in the ANSYS CFX 11 commercial code for popular test cases (low flow speed) described in literature, and then use it for verification of the in-house CFD code (created for compressible flows). The in-house CFD code has been extended lately for the Conjugate Heat Transfer modelling (CHT) as well, taking into account important flow effects, especially the turbulent transition. A Wilcox k-ω turbulence model with the Low-Reynolds modification was used in the in-house code. The calculations in ANSYS CFX were made using an SST turbulence model and a γ-Θ transition model. A fully turbulent flow was modelled by means of both codes, and the results were compared with the available experimental data. Then, the turbulent transition for several test cases was analysed with ANSYS CFX. Afterwards, the in-house CFD code was verified by means of ANSYS CFX for a higher flow speed (Mach numbers). The CHT modelling was analysed by means of both codes and the results were compared and discussed. The conducted analyses show that the results obtained by means of both codes are comparable, but the turbulence model used in the in-house CFD code is simpler and requires less computation time. A modification of two equations turbulence models can be an alternative for design problems in more developed laminar/turbulent flows.

Keywords: laminar/turbulent transition, Conjugate Heat Transfer (CHT), Computational Fluid Dynamics (CFD)

Notation

- c – specific heat capacity
- C_f – skin friction coefficient, $\tau/(0.5\varrho U_{\mathrm{ref}}^2)$
- k – turbulent kinetic energy
- l – length
- Ma – Mach number
- p – static pressure
- Pr – Prandtl number

t – time
T – static temperature
T_0 – total temperature
T_{in} – inlet static temperature
Tu_{in} – turbulence intensity
u – velocity
u^+ – near wall velocity
u – inlet velocity
U_{ref} – inlet reference velocity
x – Cartesian coordinate
y – distance to the nearest wall
y^+ – distance in wall coordinates, $\varrho y \mu_\tau / \mu$
λ – heat conductivity coefficient
μ – molecular viscosity
μ_t – eddy viscosity
μ_τ – friction velocity
ϱ – density
τ – wall shear stress
ω – specific turbulence dissipation rate

1. Introduction

Many physical phenomena have to be taken into account for proper modelling of the flow through gas turbine blade channels. The most important phenomena which are very complicated from the numerical point of view are the flow around the turbine blade and the heat transfer in the cooled blade. The correct modelling of such phenomena has a crucial influence on the core flow in the turbine, the stresses and strains in the turbine elements and in the whole turbine. Such analyses are necessary to design efficient gas turbines properly. The Computational Fluid Dynamics (CFD) is nowadays a very important tool in the development of turbomachinery. It reduces the design costs and makes it possible to better understand the physics of complex phenomena. In respect of CFD modelling, it is necessary to validate the implemented numerical methods and their application to flow configurations and geometries.

A very important issue in turbomachinery applications is the laminar/turbulent transition modelling in a boundary layer. Although, in general, the main stream in a blade passage is highly turbulent, the Reynolds number of the blade boundary layer is fairly low and the boundary layer can be either laminar or turbulent. The onset location and the extension of transition are of major importance in cases where the wall-shear stress or wall heat transfer is the object of interest.

There are mainly two modelling concepts for turbulent transition in industrial applications. The first is the use of Low-Reynolds number turbulence models, and the second is the use of experimental correlations.

In principle the Low-Reynolds transition models are calibrated to account for the effects of low turbulence intensity in the viscous sublayer. For this purpose, damping functions are introduced into the equations to achieve the desired "laminar" behaviour of the flow near the wall. This approach is not capable of enclosing many different factors that affect the transition and it is not as accurate as alternative, well-developed correlation-based models. However, it is a good alternative because of relatively easy possibilities of implementation by modifying the turbulence models and a shorter solving time.

Examples of Low-Reynolds models include the model of Wilcox [1] and the model of Langtry and Sjolander [2]. There are also many examples of investigations of the effectiveness of the Low-Reynolds models in transitional flows, for example Wilcox [3], Abe *et al.* [4], Palikaras *et al.* [5], Craft *et al.* [6] and Chen *et al.* [7].

In this paper, validation results for an in-house CFD code, which has been adapted for CHT modelling, are presented. In order to take into account the laminar/turbulent transition influence on the heat transfer, the already implemented Wilcox k-ω turbulence model has been modified using the Low-Reynolds modification [1].

This paper focuses on turbulent transition modelling and its influence on heat transfer conditions. The performed calculations are of a testing nature and their purpose has been to verify the laminar/turbulent transition modelling by means of the commercial ANSYS CFX 11 code, and to use the commercial code for verification of the academic in-house CFD code afterwards. This two-step procedure has resulted from the lack of access to experimental results for higher gas speeds (Ma > 2). It has made it impossible to test the in-house CFD code directly against experiments because the code has been created for compressible fluid flows.

2. Model definition

2.1. Geometric model and mesh

The calculations were performed with two kinds of geometry and meshes, depending on the test case. The first mesh was prepared only for a fluid domain. The flat plate was assumed as the adiabatic boundary condition. The second mesh was prepared for CHT modelling and had two domains, one for a fluid and another for a solid. The solid domain represented a flat plate 0.015 m in thickness (Figure 1).

The geometric model dimensions were scaled because of the considered test cases. Large differences in the laminar/turbulent transition location were observed, depending on the flow conditions. The numerical grid was created in a way to predict the laminar/turbulent transition correctly and to make the solutions grid independent.

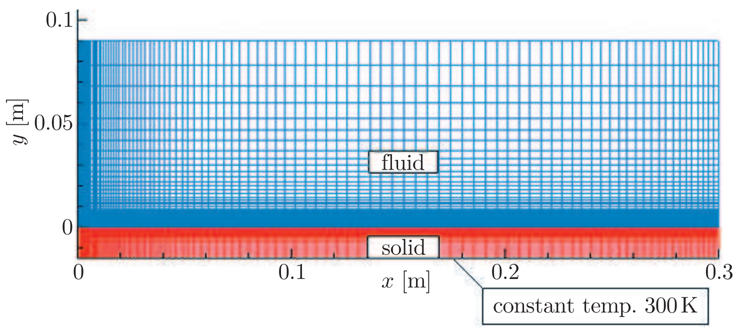

Figure 1. Example of the numerical mesh used for CHT modelling

Much attention was devoted to the mesh preparation, according to the turbulent transition modelling programme. The structural mesh parameters were set up in agreement with the ANSYS CFX Modelling Guide prescriptions [8]. The important grid guidelines are: y^+ of 1, wall normal expansion ratio 1.1 and about 75–100 nodes streamwise.

2.2. Mathematical formulation

The existing mathematical formulations and numerical schemes were used in calculations performed by means of ANSYS CFX. The SST model with a γ-Θ model for turbulent transition was used for turbulence modelling. The γ-Θ model is a two equation model, where both the intermittency and transition onset Reynolds number equations are solved. This model is a recommended transition model for general-purpose applications [8] and has been validated together with the used SST turbulence model [9–11]. This is the best solution in relation to the other models: the zero equation model with specified intermittency and the one equation model, where the transition onset momentum thickness Reynolds number is treated as a constant.

The in-house CFD code solves RANS equations. It uses the finite volume method, the MUSCL technique with a flux limiter, an upwind scheme for a convective fluxes balance, a second order finite difference scheme for a diffusive fluxes balance and integration in time with the explicit Runge-Kutta method.

The k-ω Wilcox model has been used with low-Reynolds modification for turbulence modelling in order to take into account the turbulent transition. It is an easier assumption because it does not require solving two additional partial differential equations, like in the γ-Θ model, but only a modification of the k-ω Wilcox model is required. The equations of this model are presented below and the coefficients for standard model and expressions taken into account in the transition version are presented in Table 1. The equations for k and ω can be written as follows:

$$\begin{aligned} &\frac{\partial}{\partial t}(\rho k)+\frac{\partial}{\partial x_j}\left[\rho u_j k-(\mu+\sigma^*\mu_t)\frac{\partial k}{\partial x_j}\right]=P-\beta^*\rho\omega k,\\ &\frac{\partial}{\partial t}(\rho\omega)+\frac{\partial}{\partial x_j}\left[\rho u_j\omega-(\mu+\sigma\mu_t)\frac{\partial\omega}{\partial x_j}\right]=\alpha\frac{\omega}{k}P-\beta\rho\omega^2, \end{aligned} \tag{1}$$

where:

$$\mu_t=\alpha^*\frac{\rho k}{\omega}, \tag{2}$$

$$P=\tau_{ij}^{\mathrm{turb}}\frac{\partial u_i}{\partial x_j}. \tag{3}$$

The constants Re_k, Re_ω and Re_β (Table 1) limit the range at which the coefficients α^*, α, β^* approach their fully turbulent values. The transition place and intensity can be changed by changing the values of these constants.

A complete form of the conservation of energy equation has been used for heat transfer modelling for fluids, whereas the equation is simplified for solids because

Table 1. Coefficients for standard k-ω model and expressions for low-Reynolds modification

	Standard version	Transition version
α^*	1	$\frac{\alpha_0^* + \mathrm{Re}_t/\mathrm{Re}_k}{1+\mathrm{Re}_t/\mathrm{Re}_k}$
α	5/9	$\frac{5}{9}\frac{\alpha_0 + \mathrm{Re}_t/\mathrm{Re}_\omega}{1+\mathrm{Re}_t/\mathrm{Re}_\omega}\frac{1}{\alpha_0^*}$
β^*	9/100	$\frac{9}{100}\frac{5/18+(\mathrm{Re}_t/\mathrm{Re}_\beta)^4}{1+(\mathrm{Re}_t/\mathrm{Re}_\beta)^4}\frac{1}{\alpha_0^*}$
β	3/40	3/40
σ^*	1/2	1/2
σ	1/2	1/2

$$\mathrm{Re}_t = \frac{\rho k}{\omega\mu}, \quad \alpha_0^* = \frac{\beta}{3}, \quad \alpha_0 = \frac{1}{10}, \quad \mathrm{Re}_k = 6, \quad \mathrm{Re}_\omega = 2.7, \quad \mathrm{Re}_\beta = 8$$

conduction is the only heat transfer mode in a solid. The heat conduction through the solid in CHT modelling has the following form of transport equation:

$$\frac{\partial}{\partial t}(\rho c T) = \frac{\partial}{\partial x_j}\cdot\left(\lambda\frac{\partial T}{\partial x_j}\right). \tag{4}$$

The second order finite difference scheme for heat fluxes balance has been used in the in-house CFD code.

The following algorithm has been used at the interface boundary:

- the RANS equations are solved using the fixed wall temperature;
- the balancing of solid boundary elements is performed;
- the wall temperature is calculated from the equality of heat fluxes for solids and fluids at the boundary interface;
- the steps are repeated after determining the wall temperature.

3. Results and discussion

3.1. Turbulent flow

In the first step a simple test for a fully turbulent flow was conducted. The data from the experiment of Wieghardt [12] were the basis for the test. A flow with $\mathrm{Ma} = 0.2$ was analysed. It was the limiting value for which we could perform calculations with the in-house code, created for compressible flows. Calculations were made for static pressure $p = 101\,323\,\mathrm{Pa}$ and temperature $T = 294.4\,\mathrm{K}$.

Several values have been analysed, however, for comparison purposes and by the reason of the available experimental data, dimensionless velocity u^+ related to dimensionless distance to the wall y^+ is shown (Figure 2). The results are presented in three places, close to the beginning, in the middle and close to the end of the analyzed plate. Figure 2 shows a comparison of the results obtained by means of the in-house CFD code, ANSYS CFX and experimental data. The numerical results have been compared with the analytical solution for the wall function.

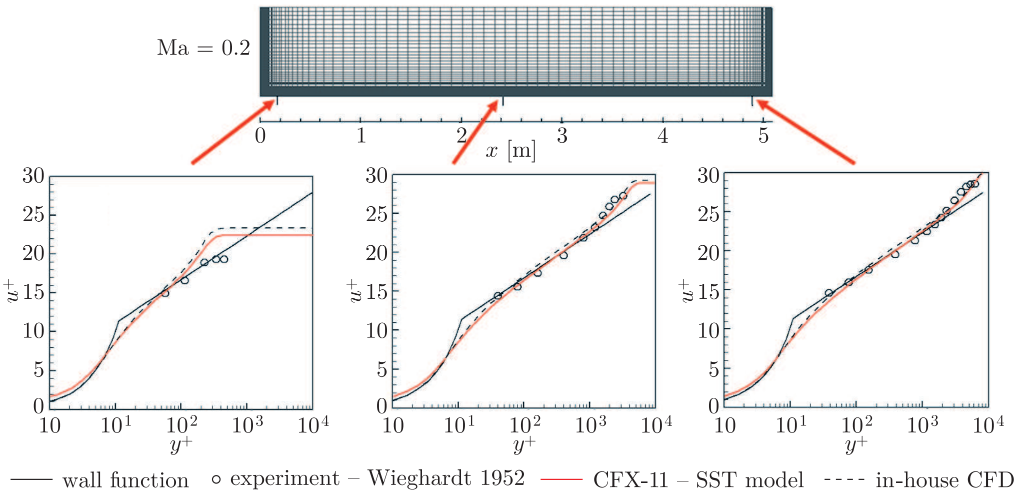

Figure 2. Results for turbulent flow calculations

3.2. Turbulent transition, ANSYS CFX – γ-Θ model

The most popular and available tests have been made for low Mach numbers. Hence, it is impossible to validate the results directly from the in-house code. At first, turbulent transition was calculated by means of ANSYS CFX to verify the approach to the problem of modelling turbulent transition with this code. It allowed us to obtain proper results for the flow with a higher Mach number and compare them with results from the in-house code.

Analyses were conducted for two test cases: T3A [13] and Schubauer and Klebanof [13]. Two analyses were conducted for the latter test, for static temperatures of $T = 290.15\,\mathrm{K}$ and $T = 871.9\,\mathrm{K}$ in order to observe the influence of temperature on the turbulent transition.

The results are presented as the skin friction C_f distribution in the dimensionless number Re_x function.

Experimental data and results obtained by means of a CFX 5 solver were available for the T3A test [9]. Thus, good conditions were provided to verify the approach to the turbulent transition modelling problem.

Calculations were made for the boundary conditions taken from the experiment: $T_{\mathrm{in}} = 290.15\,\mathrm{K}$, $u_{\mathrm{in}} = 5.4\,\mathrm{m/s}$, $\mathrm{Tu}_{\mathrm{in}} = 3.5\%$ and $\mu_t/\mu = 13.3$.

The analyses conducted for T3A test case show few differences between the calculations and experiments (Figure 3), but the situation is similar in the analysis conducted by Menter *et al.* [9] (Figure 4). It can be noticed that a small change of the velocity and turbulence intensity at the inlet would improve the convergence of the results.

The experiment of Schubauer and Klebanof [13] was used for the next analysis. Calculations were performed for the following boundary conditions: $T_{\mathrm{in}} = 290.15\,\mathrm{K}$, $u_{\mathrm{in}} = 50.1\,\mathrm{m/s}$, $\mathrm{Tu}_{\mathrm{in}} = 0.18\%$ and $\mu_t/\mu = 5.0$.

The calculation results for the Schubauer and Klebanof test case do not match the experimental data very well (Figure 5). The length on which the phe-

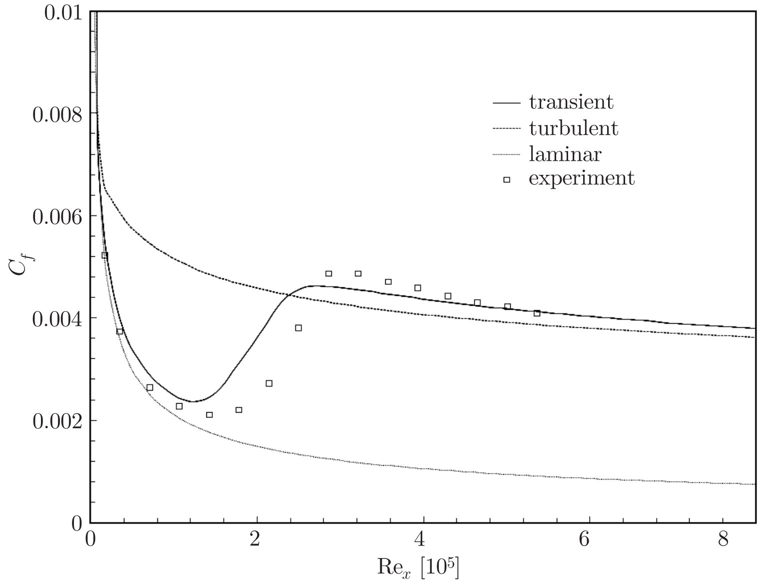

Figure 3. Skin friction for the T3A test case

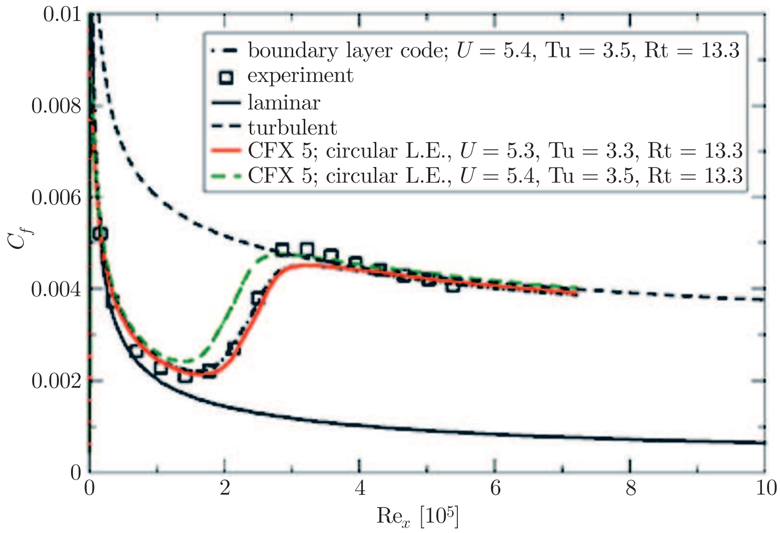

Figure 4. Skin friction for the T3A test case (literature example) [9]

nomena of transition proceeds is shorter, but the beginning of transition is modelled well. The beginning of transition on a dimensional length scale is placed on $x = 0.75\,\mathrm{m}$.

The laminar/turbulent transition for a gas turbine blade takes place at a much higher temperature. Therefore, additional calculations were made for the Schubauer and Klebanof experiment with a higher inlet temperature, $T_{\mathrm{in}} = 871.9\,\mathrm{K}$. In order to preserve the same distribution of $C_f = f(\mathrm{Re}_x)$ the plate length had to be increased. The performed analysis showed that the results related to dimensionless number Re_x were the same both for higher and lower temperature. The beginning of transition

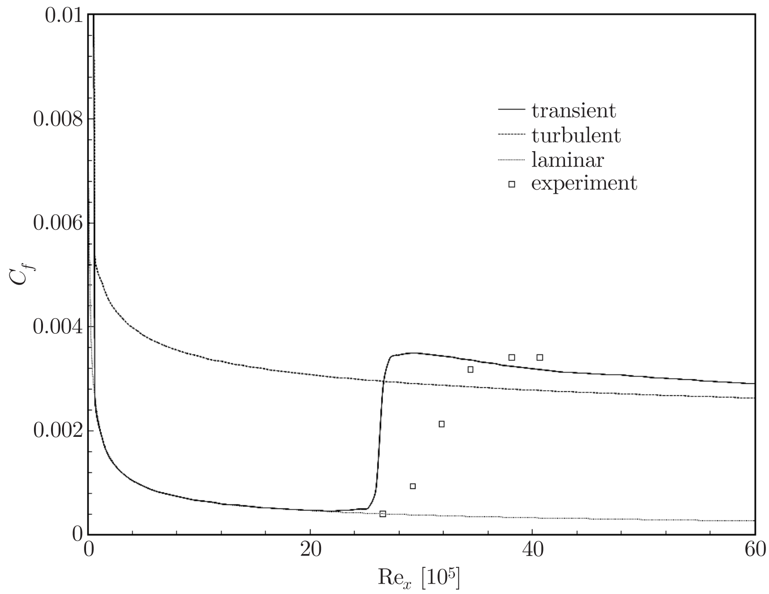

Figure 5. Skin friction for the Schubauer and Klebanof test case

for a dimensional scale was shifted more than six times streamwise. The transition beginning was placed on *ca.* $x = 4.87\,\mathrm{m}$.

3.3. Turbulent transition – CFX (γ-Θ) vs. in-house (k-ω, low-Reynolds)

The goal of the following calculations was a comparison of the results obtained by means of the in-house CFD code and ANSYS CFX. Numerical analyses were conducted for the same flat plate with Mach number $\mathrm{Ma} = 0.5$ and the inlet total temperature $T_{0,\mathrm{in}} = 873{,}15\,\mathrm{K}$. A laminar inflow on the plate was established. In that case the constants in k-ω turbulence model have the following values: $\mathrm{Re}_k = 7$, $\mathrm{Re}_\omega = 1.29$ and $\mathrm{Re}_\beta = 6$. These values have been estimated numerically to obtain the best agreement with the γ-Θ transition model.

The analysis has shown that the results obtained by means of the in-house code and ANSYS CFX are very similar, hence it may be concluded that the turbulent transition has been well modelled in the in-house code (Figure 6). It can be concluded that sufficient results for transition may be obtained using appropriate calibration of the k-ω model with the Low-Reynolds modification.

3.4. CHT modelling

According to the earlier description, a solid region was added to the geometric model for CHT modelling. The bottom side of the plate was cooled (Figure 1), it was established by constant temperature $T = 300\,\mathrm{K}$. The remaining boundary conditions were the same as in the previous case (Subsection 3.3).

Calculations were made for several materials in order to take into account different heat conductivity values. In the first case a lower heat conductivity coefficient value was assumed as $\lambda = 0.55\,\mathrm{W/mK}$, represented by glass, in the second case the calculations were made for a steel plate whose heat conductivity coefficient was much

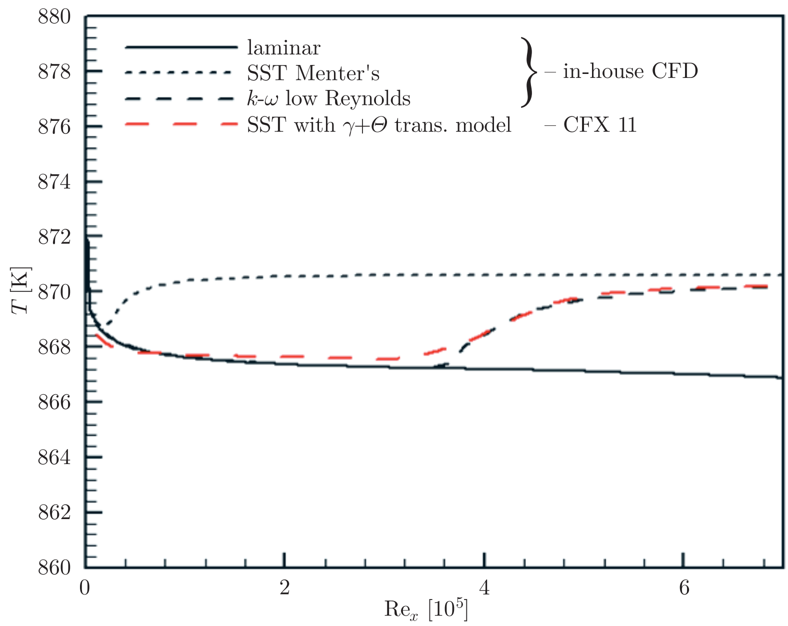

Figure 6. Comparison of results for in-house code and CFX – temperature distribution

higher, $\lambda = 60.5\,\mathrm{W/mK}$.The goal was to obtain different temperature gradients in the fluid near the wall.

The calculation results for temperature distributions, obtained by means of the academic in-house CFD code were compared with the results of ANSYS CFX. The wall temperature variation in the Reynolds number function Re_x is shown in Figure 7. It can be concluded from the results that the convergence in the laminar and turbulent area as well as in the transition area is good. The temperature profile in the near wall area is drawn (Figure 8) for a chosen point showed in Figure 7.

Glass with following properties: $\varrho = 2500\,\mathrm{kg/m^3}$, $c = 789\,\mathrm{J/kgK}$, $\lambda = 0.55\,\mathrm{W/mK}$ was used in the first calculation.

In Figure 9 the Nusselt number distribution is presented and compared with an empirical function variation for a laminar and turbulent flow. The Nusselt number range is estimated well. Small differences in the curves slope can be seen in the first section only.

In the second case, the heat conductivity coefficient has the value of $\lambda = 60.5\,\mathrm{W/mK}$, *i.e.* for steel. The other material properties are as follows: $\varrho = 2500\,\mathrm{kg/m^3}$, $c = 789\,\mathrm{J/kgK}$. A high value of the heat conductivity coefficient is the reason why the wall temperature on the fluid-solid contact region is slightly higher than the temperature on the bottom side of the plate. In this case the temperature distribution for calculations conducted by means of the in-house CFD code and ANSYS CFX are very similar (Figure 10). The temperature profile near the wall has a high gradient, its variation for a chosen point is presented in Figure 11. The temperature profile obtained by means of the academic CFD code is a little soft in nature, however, in general, it is very similar.

It can be noticed that the results obtained by means of the in-house code agree with the empirical correlation and with ANSYS CFX.

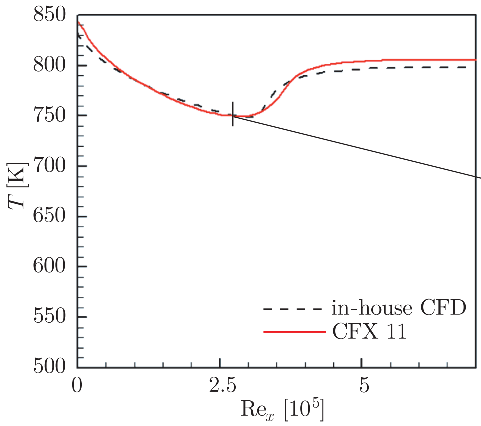

Figure 7. Temperature in function of Re_x for glass

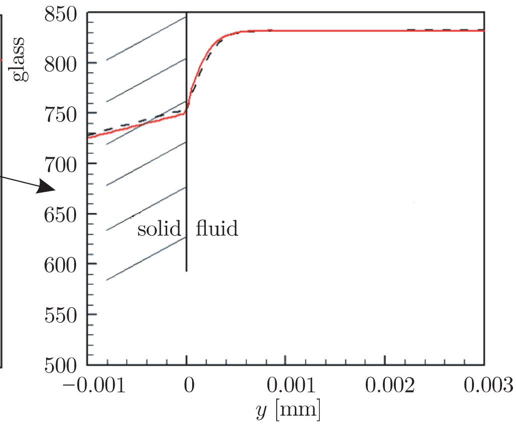

Figure 8. Temperature in normal to the boundary for glass

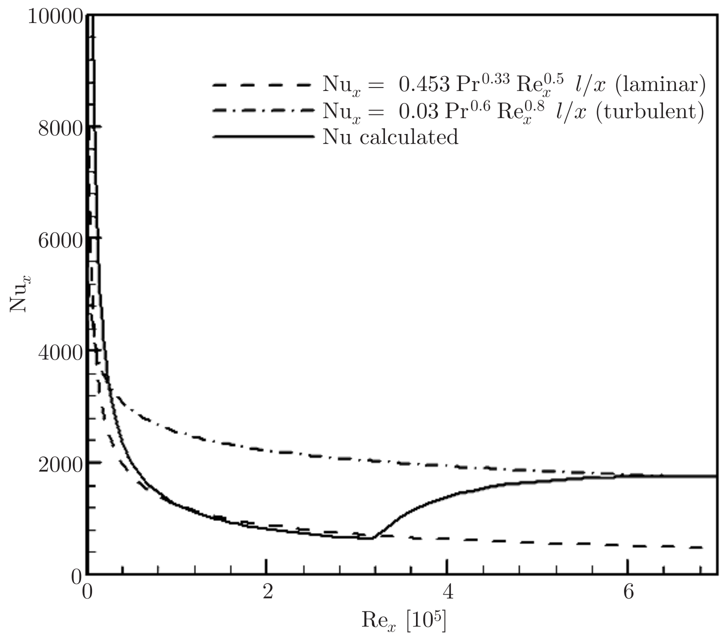

Figure 9. Nusselt number distribution in function of Re_x for glass

The distribution of the Nusselt number obtained in calculations is shown in Figure 12. The Nusselt number range is similar to that obtained from empirical formulations both in the laminar and turbulent area.

4. Conclusions

An extension of the in-house CFD code for CHT problems has been already done and tentatively validated. The fluid flow physical model is modified and includes transition modelling – an important physical process in heat transfer modelling. The Low-Reynolds k-ω Wilcox turbulence model looks promising for application of CHT

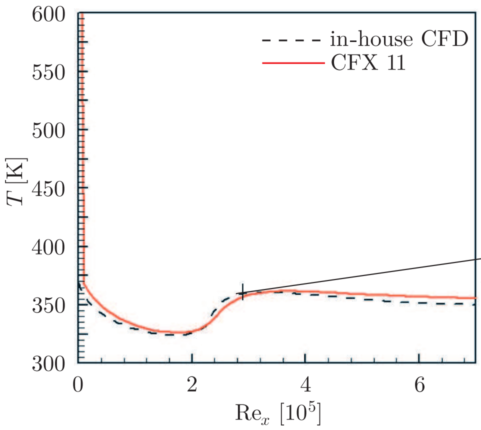

Figure 10. Temperature in function of Re$_x$ for steel

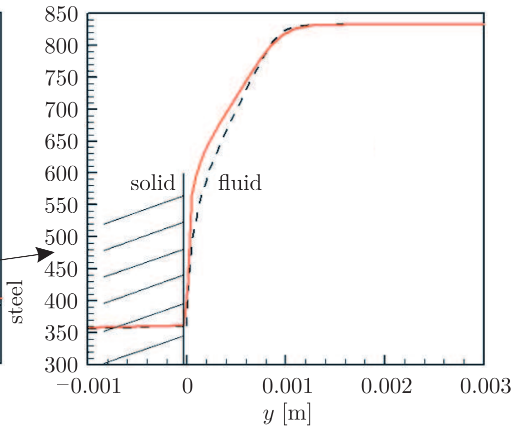

Figure 11. Temperature in normal to the boundary for steel

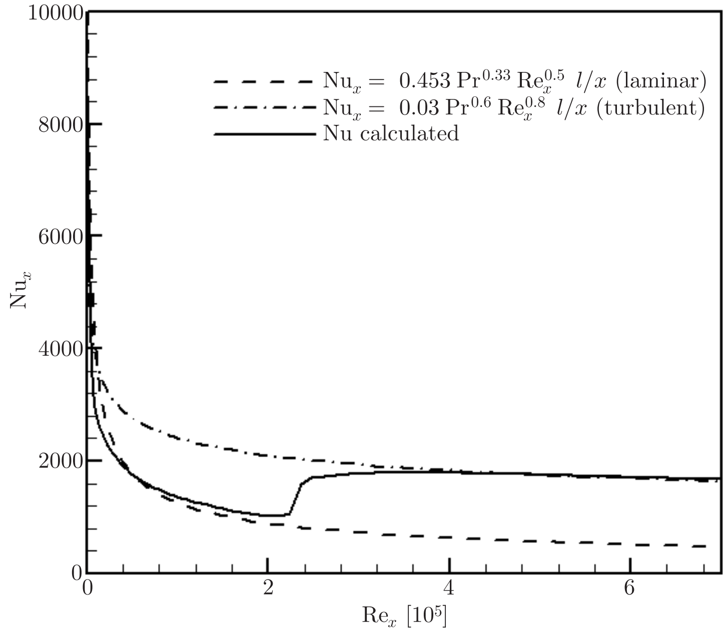

Figure 12. Distribution of Nusselt number in function of Re$_x$ for steel

calculations (due to its simplicity). All results are validated against experimental data and the commercial ANSYS CFX 11 code. The calculation results obtained by means of the in-house CFD code are comparable with the CFX 11 results. A modification of two equations turbulence models can be an alternative in the design problems for more developed laminar/turbulent flows.

References

[1] Wilcox D C 1994 *Turbulence Modelling for CFD*, DCW Industries, Inc. La Canada, Ca.

[2] Langtry R and Sjolander S 2002 *38th AIAA/ASME/SAE/ASEE Joint Propulsion Conference and Exhibit* **AIAA-2002–3643**

[3] Wilcox D C 1994 *AIAA J.* **32** (2) 247
[4] Abe K, Kondoch T and Nagano Y 1997 *Int. J. Heat Fluid Flow* **18** 266
[5] Palikaras A, Yakinthos K and Goulas A 2002 *Int. J. Heat Fluid Flow* **23** 455
[6] Craft T, Launder B and Suga K 1996 *Int. J. Numer. Methods Fluids* **17** 108
[7] Chen W, Lien F and Leschziner M 1998 *Int. J. Heat Fluid Flow* **19** 297
[8] 2006 *ANSYS CFX-Solver Modeling Guide*, ANSYS CFX Release 11.0
[9] Menter F R, Langtry R B, Likki S R, Suzen Y B, Huang P G and Völker S 2004 *ASME TURBO EXPO 2004*, Vienna, Austria **ASME-GT2004–53452**
[10] Langtry R B, Menter F R, Likki S R, Suzen Y B, Huang P G and Völker S 2004 *ASME TURBO EXPO 2004*, Vienna, Austria **ASME-GT2004–53454**
[11] Langtry R B and Menter F R 2005 *Transition Modeling for General CFD Applications in Aeronautics* **AIAA paper 2005-522**
[12] *NPARC Alliance Verification and Validation Archive*, *http://www.grc.nasa.gov/WWW/wind/valid/archive.html*
[13] *ERCOFTAC benchmark*, *http://www.ercoftac.org/*